Astron. Astrophys. 321, 363–373 (1997)

ASTRONOMY AND ASTROPHYSICS

Nebular gas abundances and mixing processes in the ringed galaxy NGC 4736⋆

P. Martin[1] **and J. Belley**[2]

[1] European Southern Observatory, Casilla 19001, Santiago 19, Chile (pmartin@eso.org)
[2] CUSLM, Université de Moncton, 165 Blvd. Hébert, Edmundston, N.-B., E3V 2S8, Canada (jbelley@novl1.ci.cuslm.ca)

Received 19 June 1996 / Accepted 20 August 1996

Abstract. Results of imaging spectrophotometry in the nebular lines Hα, Hβ, [O III] λ5007 and [N II] λ6584 of 65 H II regions in the early-type ringed galaxy NGC 4736 are presented. The oxygen abundance is derived using the line ratios [O III]/Hβ and [N II]/[O III] as calibrated by Edmunds & Pagel (1984). Analysis of the O/H distribution in the bright resonance ring of star formation in NGC 4736 reveals that the O/H scatter is similar to that of the ISM of the disc of gas-rich galaxies, despite the very high star formation rate presently observed in the ring. The magnitude of azimuthal mixing induced by supernovae explosions and galaxy differential rotation is estimated in the ring; it is found that both can explain the small O/H dispersion observed in this structure.

The radial distribution of O/H in the disc of NGC 4736 is also studied. Although the number of H II regions located outside the ring, and for which a reliable O/H value was obtained is limited, a slope for the global gradient is derived and found to be moderate ($\sim -0.035 \pm 0.020$ dex/kpc). This gradient is shallower than gradients observed in normal galaxies, and is comparable to the slopes found for galaxies with bars of medium strength. Two evolutionnary scenarios are proposed to explain this O/H distribution: *i)* Oval distortions, like bars, induce large-scale gas flows throughout the disc of NGC 4736, resulting in radial mixing of the chemical composition on a relatively short time scale ($\leq$ 1 Gyr); *ii)* A strong bar was present in the recent past and has flattened the abundance gradient.

Key words: galaxies: abundances – galaxies: evolution – galaxies: individual (NGC 4736) – galaxies: ISM – galaxies: kinematics and dynamics – galaxies: spiral

1. Introduction

Star formation and mixing processes of the interstellar medium (ISM) that are taking place in the discs of gas-rich galaxies can play a significant role in the distribution of the gas and of the heavy elements across these sytems. For instance, *radial* mixing of the ISM is present in barred spirals due to the capability of bars to transport radially large quantities of gas across galactic discs by transfer of angular momentum (e.g. Roberts et al. 1979; Athanassoula 1992; Friedli & Benz 1993; Friedli et al. 1994; Friedli & Benz 1995; Martin & Roy 1995). The easiest recognizable effect of this mechanism is seen in the oxygen abundance distribution: O/H gradients in barred galaxies are flatter than in normal galaxies (Pagel & Edmunds 1981; Vila-Costas & Edmunds 1992; Martin & Roy 1994; Zaritsky et al. 1994; Roy 1996).

Roy & Kunth (1995) have shown that mixing of the ISM by turbulent transport in the sheared flow of differential rotation can erase large *azimuthal* inhomogeneities in the chemical composition over relatively short periods of time (i.e. less than 1 Gyr). However, it is difficult to clearly identify the direct effect of azimuthal mixing in galaxies for three main reasons: 1) The abundance values derived for individual H II regions from semi-empirical methods using, for example, the nebular line ratios R_{23} = ([O II] + [O III])/Hβ, [O III]/Hβ or [N II]/[O III] , are subject to uncertainties ($\pm$ 0.2 dex) (e.g. Edmunds & Pagel 1984; Dopita & Evans 1986; McGaugh 1991). This must be deconvolved from the observed scatter of O/H abundances at a given radius in a galaxy (Walsh & Roy 1989; Kennicutt & Garnett 1996). 2) To determine the O/H dispersion, it is necessary to derive the O/H abundance for large samples ($\geq$ 50) of H II regions. 3) Gas flow patterns in the discs of spiral galaxies are complicated: in addition to the rotation shear, there can also be a radial component and local perturbations like spiral arms (Friedli et al. 1994).

One can overcome the first difficulty by *comparative* studies of the oxygen abundance distributions of a set of different galaxies, or different portions within a given galaxy (Martin & Belley 1996). For example, Martin & Roy (1995) have estimated that the scatter observed in the flat outer portion of the O/H gradient in the barred spiral galaxy NGC 3359 was greater than what is usually observed in normal or barred spirals; they concluded that azimuthal mixing had not had time to erase the large O/H

Send offprint requests to: P. Martin

⋆ Tables 3 and 4 are only available in electronic form at CDS via anonymous ftp 130.79.128.5 or via http://cdsweb.u-strasbg.fr/Abstract.html

inhomogeneities in the ISM of this galaxy, and therefore, that the bar was recent ($\tau \leq 400$ Myr).

The problem of the limited samples of H II regions can be solved by using techniques like monochromatic imaging or multi-object spectroscopy allowing large samples of H II regions (> 50) well-distributed across galactic discs (e.g. Walsh & Roy 1989; Belley & Roy 1992; Scowen et al. 1992; Martin & Roy 1992, 1994, 1995). This avenue is particularly encouraging since the ratio [N II]/[O III] now appears as reliable as R_{23} as an O/H indicator (Walsh & Roy 1989; Ryder 1995). It can be used when the [OII] 3727 line is not available, as it is the case with the monochromatic imaging techniques with narrow-band filters.

Finally one can bypass the difficulty introduced by gas flows by observing *rings* of star forming regions located near resonances in galaxies. Circumnuclear rings of H II regions are frequently observed in spiral galaxies (e.g. Wray 1988). In such rings, gas clouds are trapped in circular (or elliptical) orbits and the radial component of the velocity is significantly smaller (Combes et al. 1991; Gerin et al. 1991). Numerical models by Wada & Habe (1992) show that the large tangential shear of the gas clouds trapped in these rings (~ 100 km s^{-1}) should wipe out azimuthal abundance variations on short time scales. However, since the number of HII regions observed in nuclear rings is generally very small, it is difficult to verify this scenario. Unfortunately, abundances in circumnuclear rings are expected to be high, resulting in larger uncertainties in the O/H values due to increasing errors associated with abundance indicators as the metallicity rises (Henry 1993; Oey & Kennicutt 1993). However, simulations by Gerin et al. (1991) of velocity fields of gas clouds trapped in larger rings formed at Lindblad Resonances suggest also that azimuthal mixing of the ISM occurs on larger timescales in these structures. Thus, a more appropriate solution is to investigate the abundance distribution in large rings of H II regions found frequently, for example, in numerous barred galaxies or galaxies with oval distortions (Buta 1984; Combes et al. 1991; Buta 1995).

A ringed structure very well-suited for conducting such a study is found in the RSAab(r) galaxy NGC 4736. In this paper, we present the results of an abundance survey using interference filters to study the O/H distribution in this star-forming ring galaxy. Since there is a considerable interest in establishing the chemical composition in galactic discs, in particular in early-type spirals (see Sect. 3.3), the radial O/H gradient of NGC 4736 is also discussed. In Sect. 2, we examine some morphological and kinematical properties of NGC 4736 and we present the observations and image analysis. In Sect. 3, the O/H distribution in the star-forming ring is presented and the global O/H gradient in the disc of NGC 4736 is discussed. We show that the apparent O/H dispersion in the ring is small and similar to the spreads observed in the well-mixed ISM of discs of normal gas-rich galaxies like NGC 628. Also, the slope of the global O/H gradient appears significantly shallower than the slope measured in normal disc galaxies of similar type. Azimuthal and radial mixing processes in NGC 4736 are discussed in Sect. 4, and we suggest also two possible evolutionary scenarios to explain the actual radial distribution of the chemical composition in this galaxy.

2. Observations

2.1. NGC 4736: general morphology and properties

NGC 4736 (M94) is a very well-studied object, the main reason being the presence of multiple ring-shaped structures observed in the galaxy (e.g. Bosma et al. 1977; Buta 1984; Buta 1988). It is a member of a nearby group of galaxies but shows no obvious signs of a recent close encounter with another galaxy. Throughout this paper, we will assume a distance of 6.3 Mpc ($1'' = 30.5$ pc) (Gerin et al. 1991). The most spectacular feature is the very bright inner ring of numerous H II regions located at R $\sim 45''$ (axis ratio ~ 0.73) (Sandage 1961; Lynds 1974; Buta 1984; Pogge 1989; Wray 1988; Sandage & Bedke 1994; Fig. 1). A bright central region (R $\sim 15''$) and spiral arm structure are bounded by this ring. A faint outer ring is observed far from the center (R $\sim 330''$) on long exposure plates (e.g. Mulder & van Driel 1993). Recently, Huang et al. (1994) have claimed that a third inner ring (at about $5''$) and a short bar are present in deep V-band images. This nuclear bar ($a \sim 15''$) had been found previously by Shaw et al. (1993) in their near-IR images. This bar was recently studied by Möllenhoff et al. (1995); they showed that this structure does not have a strong dynamical influence on the hot stellar component, but induces non-circular motions in the gas in its vicinity. However, contrary to the frequent cases where star formation is very active around the nucleus of galaxies with nuclear bars (Wozniak et al. 1995), star formation in the central region of NGC 4736 is mostly absent (Möllenhoff et al. 1995). The ratio of the infrared over the Hα emission in the nucleus is 100 times higher than in the inner ring (Gerin et al. 1991). According to Walker et al. (1988), the nucleus of NGC 4736 may be in a post starburst phase and the discovery of several compact supernovae remnants in the nuclear region by Duric & Dettmar (1988) tends to confirm that star formation activity was certainly high in the recent past. Maoz et al. (1995) have shown that the very compact UV source found at the position of the optical center is a LINER; they suggest that NGC 4736 could be in the final stages of a merger.

Neutral hydrogen gas has been mapped by Van der Kruit (1971), Bosma et al. (1977), de Bruyn (1977), Klein & Emerson (1981), Gioia & Fabbianno (1987), Condon (1987) and Mulder & van Driel (1993). The latter authors have demonstrated that the H I kinematics show evidence for the presence of an oval distortion. However, no strong streaming motions of gas are observed in the disc but peculiar velocities are present at the location of the inner ring. CO observations of NGC 4736 were published by Gerin et al. (1991). They found that the molecular gas is kinematically similar to the H I and were able to reproduce the CO distribution assuming that the galaxy is a massive oval of axial ratio of 0.8.

The O/H abundances have been derived in nine H II regions in the ring and the disc of NGC 4736 by Oey & Kennicutt (1993) using the indicator R_{23} as calibrated by Dopita & Evans (1986).

Table 1. General properties of NGC 4736

Parameter	Value
α (1950) [a]	$12^h\ 48^m\ 32^s$
δ (1950) [a]	$41^\circ\ 23'\ 28''$
Morphological type [a]	RSAab(r)
Inclination [b]	40°
Position angle [b]	294°
B_T^0 (mag) [a]	8.72
Galactic Extinction (B) [c]	0.00
v (km s^{-1}) [d]	308
R_{eff} (arcsec) [a]	77
D (Mpc) [e]	6.3
Scale (pc arcsec^{-1})	30.5

Notes: (a) De Vaucouleurs et al. 1991; (b) Mulder 1995a; (c) Tully 1988; (d) Mulder & Van Driel 1993; (e) Gerin et al. 1991.

They found a slope for the O/H gradient of -0.017 dex/kpc which is considerably flatter than the slopes derived in normal spirals using the same indicator and O/H calibration (e.g. NGC 2997 studied by Walsh & Roy 1989); because only two H II regions were observed outside the inner ring, the uncertainty on the slope is considerable. The general properties of NGC 4736 are given in Table 1.

2.2. Observations

In order to study the O/H abundance distribution of a large sample of H II regions in the ring and the disc of NGC 4736, we employed a monochromatic imaging technique using interference filters. This method has been extensively described by Belley & Roy (1992), Scowen et al. (1992), Martin & Roy (1992, 1994, 1995) and Roy et al. (1996). Observations were carried out using a focal reducer (f/8 $\rightarrow$ f/3.5) on the Mont Mégantic Observatory 1.6 m telescope in May 1993. The detector was a Thomson 1024 $\times$ 1024 CCD with a pixel size of 0.7″. With this configuration, the useful field of view is about 9 arcmin in diameter, covering most of the optical disc of NGC 4736. A set of narrowband ($\Delta\lambda$ = 10 or 20 Å) filters was used to observe the galaxy in the main nebular lines Hα, Hβ, [O III] λ5007 and [N II] λ6584. Visual and red continua images were obtained using two other filters with broader bandpasses (200 Å) centered at 5370 Å and 7020 Å, respectively. The bandpass of the narrower filters was adjusted to match the redshifted nebular lines of NGC 4736 by tilting the filters and compensating for the blueshift introduced by low outdoor temperatures. Observations were performed as sequences of several exposures of 3000-4000 s for each of the narrow-band filters, and of 1000 s for the continuum filters. The journal of observations of NGC 4736 is given in Table 2.

Table 2. Journal of observations

Period	Line	Filter (Å)	FWHM (Å)	Integration time (s)
1993 May 15	Visual	5370	200	3×1000
1993 May 15	Red	7020	200	3×1000
1993 May 15	Hα	6577	10	3×3000
1993 May 17	[O III]	5019	10	3×4000
1993 May 19	Hβ	4872	10	3×3000
1993 May 19	[N II]	6602	10	3×3000

2.3. Image analysis

Image reduction and analysis were performed with IRAF[1] following usual procedures described in Belley & Roy (1992), Scowen et al. (1992) and Martin & Roy (1992). The CCD used has an important dark current which is the main source of noise in our long exposure images. Dark counts were evaluated in non-exposed sections of the detector for each image and subtracted. Flatfielding was achieved using a set of high S/N dome flats obtained with the same setup as the astronomical images. The resulting images show that the amplitude of the residual large-scale variations across the CCD field is reduced to about 2%.

The subtraction of the galaxy stellar continuum was performed by using a scaling factor between the emission-line and continuum images estimated from several stars in the field. The final subtraction was obtained after adjusting this factor by small amounts to avoid bumps or hollows in the vicinity of the galactic nucleus, in the spiral arms and in the ring-shaped structure. The monochromatic image of NGC 4736 at Hα is presented in Fig. 1; the image showing the stellar continuum at 5370 Å is presented in Fig. 2.

Integrated fluxes and accurate positions of H II regions in NGC 4736 were measured interactively by using small squared windows of different sizes matching the angular dimension of the regions. From these measurements, the line ratios Hα/Hβ, [O III]/Hβ and [N II]/[O III] were calculated. A calibration factor derived from the spectrum of one bright small H II region obtained with the multi-object spectrograph (MOS) at the CFHT (identified as No.13 in Fig. 3 below) was then applied to these line ratios. A comparison of the calibrated [O III]/Hβ ratios of several H II regions in common with Oey & Kennicutt (1993) reveals good agreement ($\sim$ 10%). Flux ratios of the H II regions were then corrected for the interstellar reddening from comparison of the Hα/Hβ ratio with the theoretical Balmer decrement (Case B) as given by Osterbrock (1989) for a density of 100 cm^{-3} and a nebular temperature of 8000 K. The reddening correction was applied using the reddening law formulated by Savage & Mathis (1979) and was performed after correcting the observed Hβ fluxes by adding 2 Å of equivalent width to the Hβ to compensate for the underlying Balmer absorption. This last

[1] IRAF is distributed by National Optical Astronomy Observatory which is operated by the Association of Universities for Research in Astronomy, Inc, under contract to the National Science Foundation

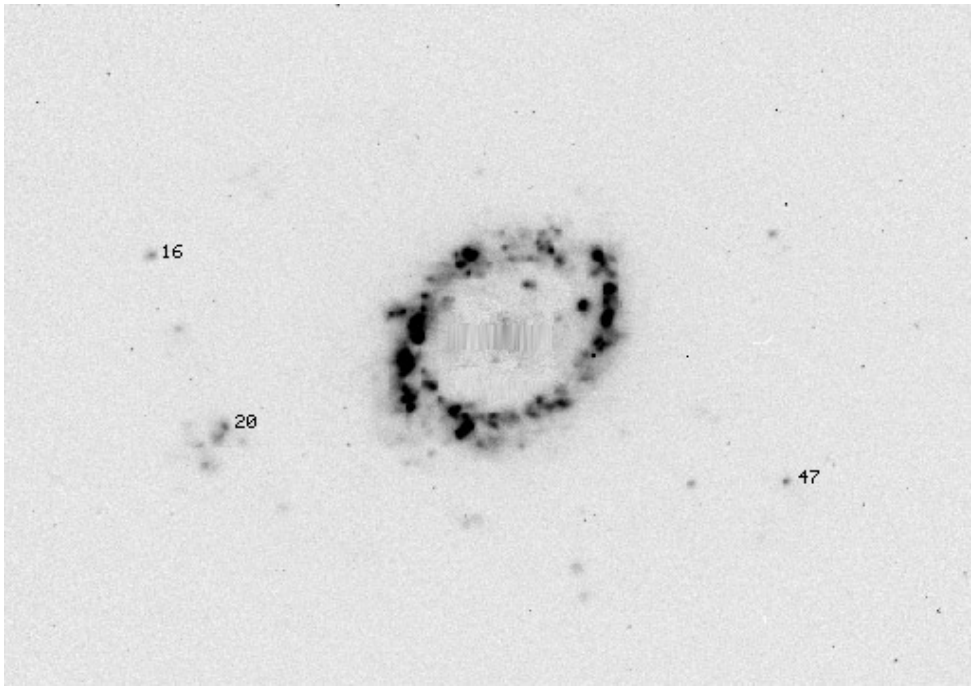

Fig. 1. Hα image of the ringed galaxy NGC 4736, obtained with the Mont Mégantic 1.6m telescope, showing the rich population of H II regions present in the inner ring as well as a few star-forming regions in the disc. The field shown is about 6.7 $\times$ 4.7 arcmin^2. The artifact in the center was caused by the saturation of the subtracted red continuum image. North is at the top, and east is at the left.

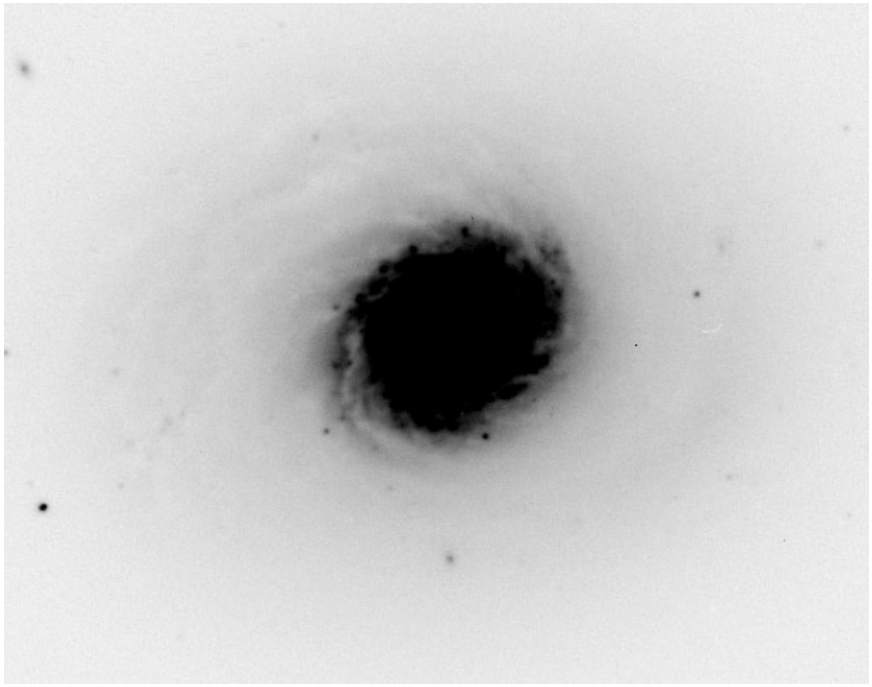

Fig. 2. Visual continuum image (5370 Å, $\Delta\lambda$ = 200 Å) of the galaxy NGC 4736. The very bright bulge and the low surface brigthness disc are clearly visible. Field and orientation are as in Fig. 1.

correction corresponds to the average value found by McCall et al. (1985) in a study of H II regions in the discs of a large sample of spirals; this value was found to be appropriate for the spectra of the H II regions in NGC 4736, as described by Oey & Kennicutt (1993).

3. Results

3.1. The sample of H II regions

In the initial sample, fluxes for 88 H II regions were measured in all the spectral lines observed. All H II regions with S/N $\geq$ 5 at Hβ, [O III] and [N II] were then retained for spectrophotometry; 17% of the initial sample was rejected because low detection at Hβ and another 9% because the [O III] line was too weak.

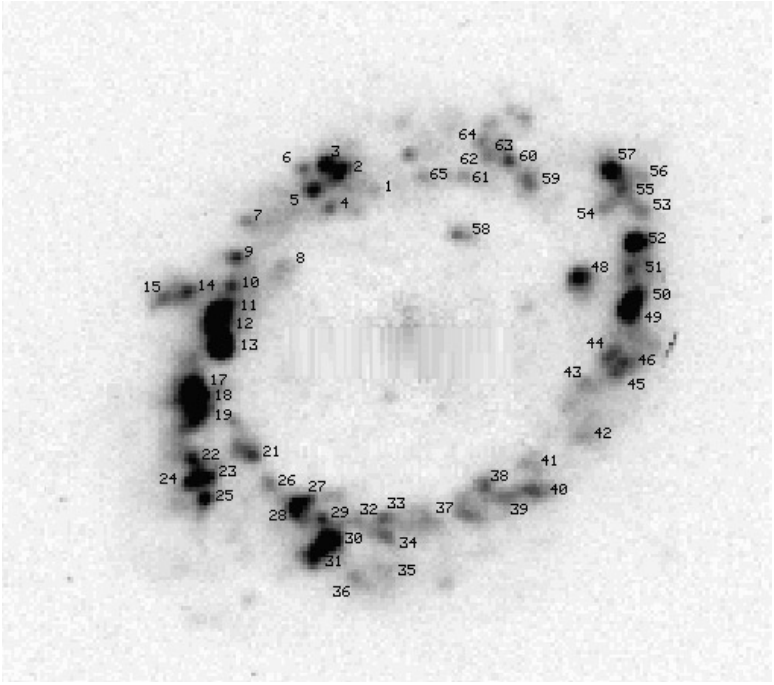

Fig. 3. Hα image of the inner ring of star formation in NGC 4736. Numbers identify the H II regions for which a reliable value of the O/H abundance was derived. The field is about 2.4 $\times$ 2.4 arcmin^2 ; north is at the top, and east is at the left.

The final sample of 65 H II regions is listed in Table 3. The positions X and Y with respect to the galaxy center are given in arcseconds (north and east are positive). In the last column, "AP" refers to the size of square apertures used to measure the integrated fluxes. Three window sizes were applied corresponding to 4, 12 and 24 arcsec^2 as indicated by the numbers 1 to 3, respectively. The individual H II regions in the ring and for which O/H values were derived are identified on the Hα image in Fig. 3; regions outside the ring are labeled in Fig. 1.

The de-reddened [O III]/Hβ and [N II]/[O III] line ratios, the galactocentric distance corrected for the galaxy inclination and the logarithmic extinctions at Hβ of H II regions in NGC 4736 are given in Table 4. The ratio [O III]/Hβ is defined as 1.35I([O III] λ5007)/I(Hβ) and [N II]/[O III] as I([N II] λ6584)/I([O III] λ5007). Uncertainties given are 1σ errors derived from the original CCD images and propagated through arithmetic operations. Several negatives values of c were found and set to zero (errors on c were not propagated). The Galactic value of extinction (B band) in the direction of NGC 4736 is negligible (0.0 mag. according to Tully 1988).

3.2. The O/H distribution in the inner ring

The oxygen abundance of the H II regions in NGC 4736 can be derived using semi-empirical relationships between O/H and specific nebular line ratios (e.g. Edmunds & Pagel 1984; Dopita & Evans 1986; McGaugh 1991). Intrinsic uncertainties due to these empirical methods are estimated at $\pm$ 0.2 dex on individual points. However, these uncertainties are more important for high-metallicity regions, that is, higher than solar metallicity which is 12 + log(O/H) = 8.9 (Oey & Kennicutt 1993; McGaugh 1991). The O/H values in the ring of H II regions in NGC 4736 are very close of the solar value (Oey & Kennicutt 1993; this paper) suggesting that the uncertainties are probably not much higher than $\pm$ 0.2 dex. This is important for the comparative analysis of the O/H spread in the ring with the scatters observed in the discs of Sc galaxies described below since the average O/H value in these last objects is generally close or lower than the solar value.

Two indicators, [O III]/Hβ and [N II]/[O III], calibrated by Edmunds & Pagel (1984) were used to derive the O/H abundances in NGC 4736. The values are given in the last columns of Table 4. The O/H distributions in the star-forming ring, obtained with both O/H indicators, are illustrated in Fig. 4. One can see that the *apparent* dispersion are much smaller (by about 30%) for the abundance distribution obtained with the [N II]/[O III] ratio than with [O III]/Hβ (see Table 5 below for quantitative data); this was already noticed by Belley & Roy (1992) and is explained by the fact that [N II]/[O III] is less sensitive to certain physical conditions of the nebulae like the effective temperature and the ionization parameter (Martin & Roy 1995). Thus, to compare the O/H distributions between different galaxies, it is imperative to employ the *same* abundance indicator and calibration. Recent works (Ryder 1995; Roy & Walsh 1996) have shown that the [N II]/[O III] ratio is a more reliable O/H indicator than [O III]/Hβ , although more affected by dust extinction. For this last reason, we will used O/H values derived from both indicators to conduct our comparative analysis.

Fig. 5 illustrates the apparent O/H abundance dipersions observed in the disc of four spiral galaxies: NGC 628 and NGC 6946 (Belley & Roy 1992); NGC 925 and NGC 1073 (Martin & Roy 1994). All these data were obtained with the monochromatic imaging technique. For concision, only the O/H values derived with the line ratio [N II]/[O III], calibrated with Edmunds

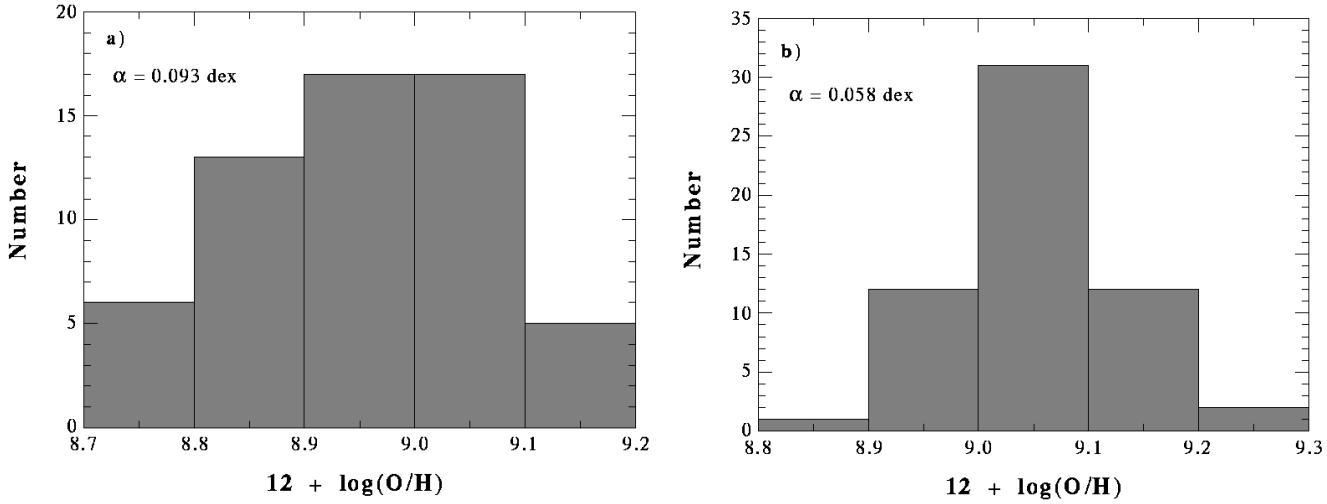

Fig. 4a and b. Oxygen abundance distribution in the inner ring of NGC 4736. **a** The O/H values were derived using the [O III]/Hβ ratio (Edmunds & Pagel 1984); **b** The [N II]/[O III] ratio was used as the O/H abundance indicator (Alloin et al. 1979).

& Pagel (1984), are presented. Mean deviations (α) are given for each diagram. More quantitative data, including the O/H dispersions when [O III]/Hβ is employed as the abundance indicator, are presented in Table 5. Except for both barred spirals (NGC 925 and NGC 1073), the radial ranges selected for deriving the O/H dispersions are small ($\sim 0.2R_{eff}$). Larger ranges were required for the barred galaxies in order to increase the number of H II regions (N) for statistically significant O/H dispersions. Since the O/H gradients in both objects are shallow, the error introduced by the *radial* variation of O/H in the scatter is negligible ($\sim$ 0.02 dex). These data and a comparison of Fig. 5 with Fig. 4 reveal that *the apparent O/H dispersion in the star-forming ring of NGC 4736 is comparable with the spread observed in the disc of gas-rich galaxies (even slightly smaller when* [N II]/[O III] *is used as the abundance indicator).*

3.3. The global O/H gradient

Radial abundance gradients are a common feature in the discs of spiral galaxies and a fundamental clue to understand galaxy evolution. Differences in the radial distribution of the metals between distinct morphological types of galaxies are now clearly recognized. Belley & Roy (1992), Vila-Costas & Edmunds (1992), Edmunds & Roy (1993), Zaritsky et al. (1994) have shown that all late-type (Sc) *unbarred* galaxies exhibit strong O/H gradient of similar amplitude (slope $\sim 0.09 \pm 0.02$ dex/kpc). Furthermore, it is now well established that the presence of a bar affects significantly the distribution of the chemical composition in galactic systems: abundance gradients in barred spirals are *shallow* and their slope is related to the axis ratio of the stellar bar (Martin & Roy 1994). Moreover, Oey & Kennicutt (1993) have suggested that the O/H gradients in early-type spirals are flatter than in late-type objects but this result needs further confirmation, because only a few H II regions were observed in each galaxy of their sample. Very low-mass galaxies and magellanic irregulars do not have abundance gradients at all (Pagel et al. 1978; Pagel et al. 1980; Roy et al. 1996). Because its morphology is representative of a whole class of ring galaxies (and also since it is an early-type spiral), there is an interest in studying the global O/H distribution in the disc of NGC 4736 and in trying to relate it to the behavior in other morphological types.

Despite the faintness of the H II regions outside the inner ring, we were able to derive reliable O/H values for a few of them (identified on Fig. 1). The global O/H gradients in NGC 4736, derived with both [O III]/Hβ and [N II]/[O III] indicators, are illustrated in Fig. 6. For both ratios, the inferred gradients obtained have an identical slope: $-$ 0.033 dex/kpc and $-$ 0.035 dex/kpc for [O III]/Hβ and [N II]/[O III], respectively. Two other regions located in the disc (+118$-$41;+124$-$52), not identified in Fig. 1, are shown in these diagrams (open symbols). These regions were not included in the final sample since the S/N ratios for their Hβ emission line were just under the threshold fixed for the final selection. The dashed-line regressions shown in Fig. 6 were obtained in taking into account these H II regions. When both points are added, the slopes become steeper: $-$ 0.050 dex/kpc and $-$0.054 dex/kpc. These values are significantly higher than the slope ($-$ 0.017 dex/kpc) obtained by Oey & Kennicutt (1993) using the R_{23} indicator and the calibration of Dopita & Evans (1986). Walsh & Roy (1989) and Kennicutt & Garnett (1996) have shown that O/H gradients obtained with this calibration are shallower by about a factor of two when compared with gradients established from the calibration of Edmunds & Pagel (1984). If we applied this last calibration to Oey & Kennicutt data, the slope becomes significantly steeper: $-$0.042 dex/kpc. Given the very few number of points outside the inner ring for which the O/H abundance was derived, it is also not surprising that the gradient slope is severely affected when another calibration is employed. In our case, the steepness of the gradient comes from the last point at R = 5.1 kpc; without

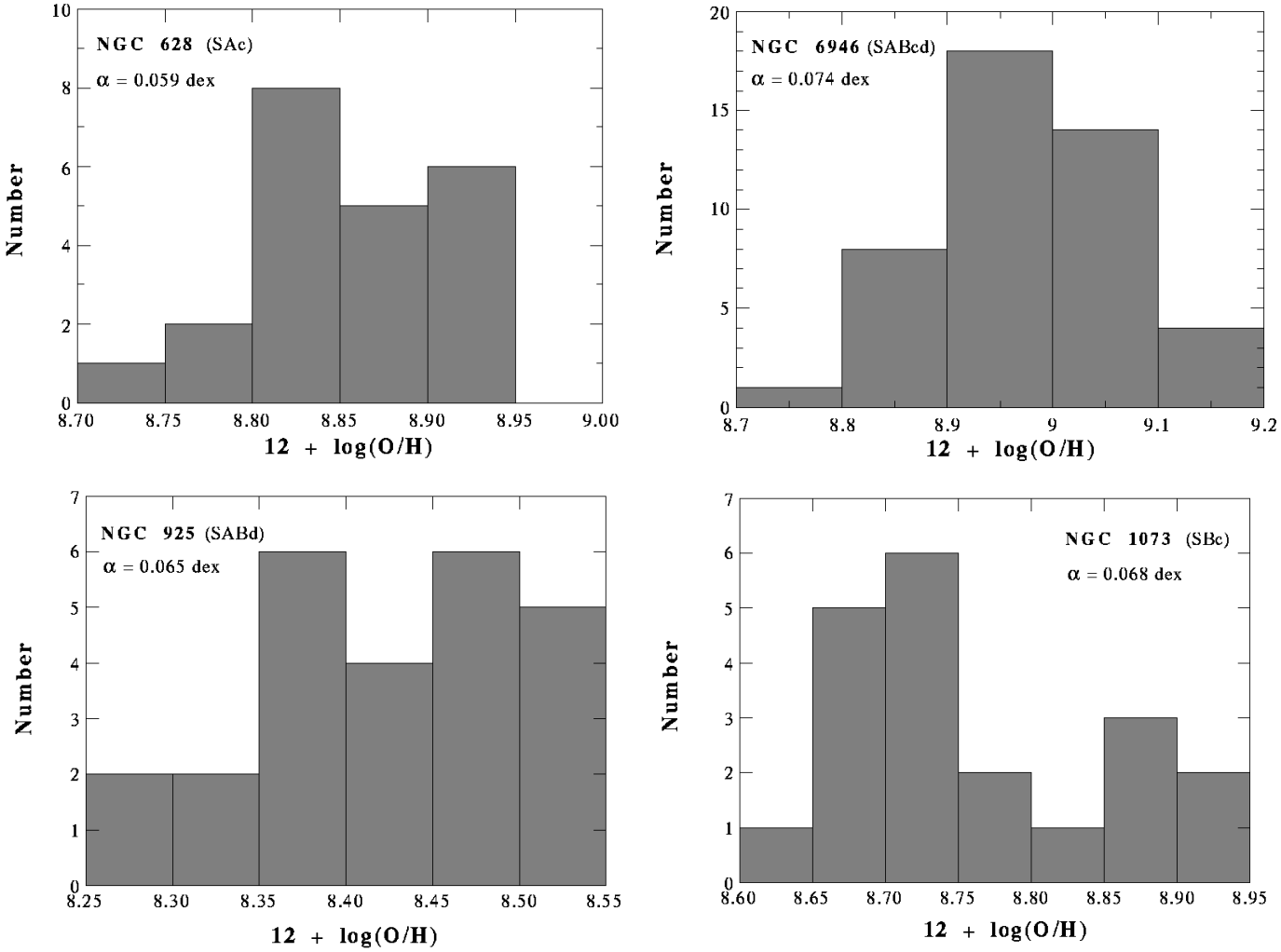

Fig. 5a–d. Apparent O/H dispersions for four spiral galaxies (see also Table 5). The O/H values were obtained with the [N II]/[O III] ratio, calibrated by Edmunds & Pagel (1984).

Table 5. O/H dispersions*

Galaxy	Radial range (R/R_{eff})	N	$(O/H)_{min}$	$(O/H)_{max}$	$\langle O/H \rangle$	α (dex)	σ (dex)
NGC 628	1.01 – 1.19	26	8.51	9.01	8.78	0.091	0.117
		24	8.69	9.00	8.86	0.059	0.072
NGC 925	0.65 – 1.20	29	8.23	8.79	8.51	0.106	0.129
		25	8.26	8.53	8.42	0.065	0.079
NGC 1073	0.55 – 0.90	21	8.39	8.77	8.55	0.082	0.105
		20	8.63	8.91	8.76	0.068	0.083
NGC 4736	0.45 – 0.72	58	8.72	9.19	8.95	0.093	0.114
		58	8.83	9.23	9.06	0.058	0.079
NGC 6946	0.60 – 0.80	45	8.69	9.22	9.00	0.097	0.120
		45	8.71	9.19	8.97	0.074	0.095

$\star$: For each object: the first line gives the O/H properties derived from [O III]/Hβ ; second line: O/H abundances derived from [N II]/[O III]

Table 6. O/H gradients in a sample of spiral galaxies

Galaxy	Type[a]	N[b]	ϵ_b	Gradient[c]	Reference
NGC 628	SA(s)c	130	0	−0.081	1
NGC 925	SAB(s)d	82	4	−0.033	2
NGC 1073	SB(rs)c	55	7	−0.048	2
NGC 1365	SB(s)b	19	6	−0.020	3
NGC 2997	SAB(rs)c	49	2	−0.093	4
NGC 3184	SAB(rs)cd	49	1	−0.101	5
NGC 4303	SAB(s)cd	79	4	−0.073	6
NGC 4736	RSAab(r)	65	2	−0.033	7
NGC 5457	SAB(rs)cd	248	2	−0.109	8
NGC 6946	SAB(rs)cd	160	1	−0.089	1

Notes: (a): De Vaucouleurs *et al*. 1991 (RC3); (b): Number of sampled H II regions; (c) Slope in dex kpc^{-1}

References: (1): Belley & Roy 1992; (2): Martin & Roy 1994; (3): Roy & Walsh 1996; (4) Walsh & Roy 1989; (5) Martin 1992; (6) Martin & Roy 1992; (7) This work; (8) Scowen *et al*. 1992.

this point, the gradient becomes shallower (−0.015 dex/kpc). The addition of the above two H II regions tends to confirm, however, that the O/H value derived for this region is correct. In short, the slope of the gradient in NGC 4736 is $\sim -0.035 \pm 0.020$ dex/kpc.

Nevertheless, although the exact value of the O/H gradient slope in NGC 4736 remains uncertain, a definitive result emerges: *the gradient is significantly shallower than normally observed in large late-type spiral galaxies*. In fact, according to the relationship between the slope of the O/H gradient and the bar ellipticity (i.e. $\epsilon_b = 10(1 - b/a)$ where b/a is the axis ratio of the stellar bar) found by Martin & Roy (1994), the gradient in NGC 4736 is rather similar to the ones observed in moderately barred galaxies ($\epsilon_b \sim 4$) (Table 6). However, NGC 4736 does not possess a strong barred structure, but has instead a massive oval distortion and a short nuclear bar. In Sect. 4.2, we will explore two possible evolutionnary scenarios to explain the shallow gradient.

4. Discussion

4.1. The O/H dispersion in the star forming ring

In Sect. 3.2, we have shown that the apparent O/H dispersion in the star-forming ring of NGC 4736 is similar to the scatter observed in the disc of other gas-rich spirals. However, there is an ongoing debate about the apparent dispersion of abundances observed in galaxies: is it real or the result of uncertainties introduced by the calibrations or by variations in nebular structure and ionization properties? Since the apparent O/H dispersion in NGC 4736 is significantly smaller when [N II]/[O III] is employed as an abundance indicator, this suggests that a large part of the dispersion observed when the [O III]/Hβ ratio is used is not related to a real variation in abundance. Recently, Kennicutt & Garnett (1996) have investigated this issue in their extensive study of nebular abundances in M101. They have concluded that the O/H abundance scatter in this galaxy, derived from the R_{23} indicator calibrated by Dopita & Evans 1986, is probably overestimated. Thus, a priori, it is difficult to justify a direct comparison of the azimuthal O/H distribution between different galaxies since the real dispersion in abundance is uncertain.

However, some physical arguments can be employed to show that azimuthal mixing is effective in the star-forming ring of NGC 4736, even if the real O/H scatter is not known. From Hα observations, Kennicutt (1983) has derived a global star formation rate of $\sim$ 1.4 M$_\odot$/yr in NGC 4736. In comparison, the total SFR in the normal spiral galaxy NGC 628 is about 8.4 M$_\odot$/yr. However, contrary to NGC 4736, star formation is present across the whole disc of NGC 628. The surface covered by the ring in NGC 4736 is approximately 1/150 of the area of the entire disc of NGC 628 (assuming a distance of 7 Mpc for NGC 628). Thus, the SFR per unit area is about 25 times higher in the ring of NGC 4736 than in the disc of NGC 628. Assuming that the IMF in the ring of NGC 4736 and the disc of NGC 628 are the same, we could expect a much higher rate of supernovae explosions per unit area in the former galaxy. According to Edmunds (1975) and Roy & Kunth (1995), continuous massive star formation in galactic discs and the resulting supernovae explosions are the sources of different hydrodynamical mechanisms that induce mixing of the chemical composition of the ISM. According to the simulations of Gerin et al. (1991), star formation in the ring of NGC 4736 is active since at least 1 Gyr. For a continuous star formation model, the O/H variations $\propto 1/\sqrt{n}$, where n is the number of supernovae events (Edmunds 1975). Although this model is over-simplistic (see Roy & Kunth for a complete discussion), when applied to NGC 4736, it suggests that supernovae-induced mixing can wipe out large O/H inhomogeneities in the ring of massive star formation in $\sim$ 100 Myr.

Recently, Tenorio-Tagle (1996) has argued that mixing of the new elements of hot material ejected from type II supernovae with the cold phase ISM takes place only after cooling of the ejecta over long periods of time (a few 100 Myr). True mixing occurs only when the metal-rich "droplets" have cooled down and fell back onto the disc of the galaxy. The enriched droplets are then disrupted by photoionization from new generations of massive stars and the chemical composition of the ISM is finally changed. If massive star formation plays such an important role in mixing the ISM, the absence of large O/H inhomogeneities in the ring of NGC 4736 is then not too surprising.

According to the preceding scenarios, we could then expect a difference in the azimuthal O/H distributions in the ring and in the rest of the disc since star formation is mostly absent in the latter. However, given the very small number of H II regions in the disc of NGC 4736, this hypothesis will be difficult to prove.

On a larger scale, other mixing mechanisms are acting (Roy & Kunth 1995). For instance, in a galaxy with a radial gradient in velocity S due to differential rotation, the time scale for azimuthal mixing by turbulent diffusion is given by

$$\tau_{x_{az}} = \frac{\Delta x_{az}^{2/3}}{S^{2/3} v^{1/3} l^{1/3}} \quad (1)$$

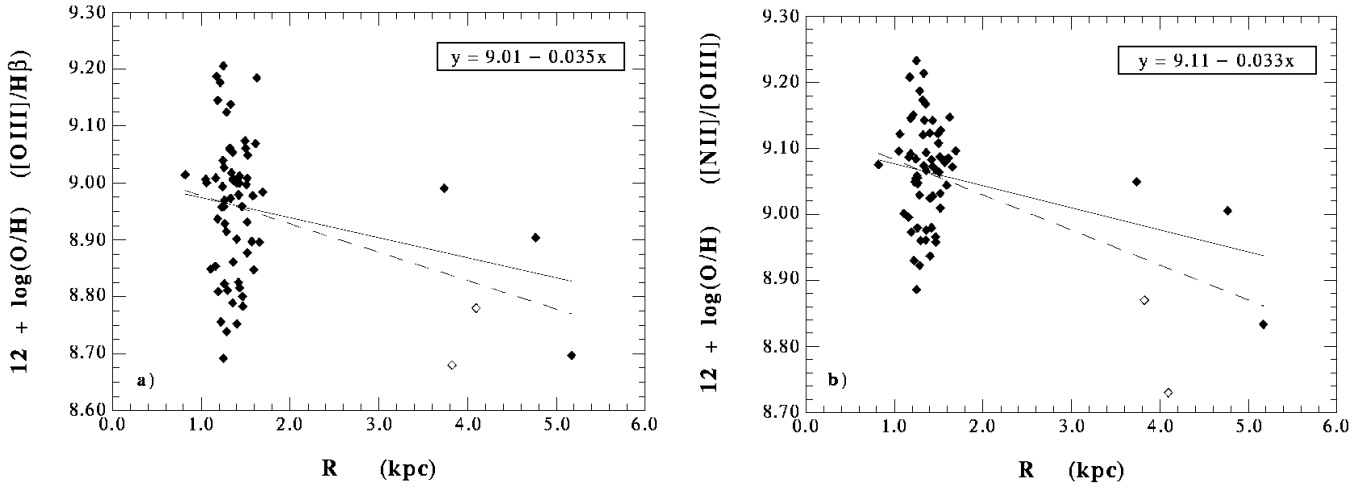

Fig. 6a and b. The global O/H abundance gradient in the ringed galaxy NGC 4736. **a** Gradient derived when the [O III]/Hβ ratio is used as the O/H abundance indicator. **b** Gradient derived when [N II]/[O III] is employed as the O/H abundance indicator. Full lines and equations of correlation represent the fits obtained with only three H II regions observed outside the inner ring. Dashed lines are the regressions obtained when two other outside regions (open symbols) are added.

where Δx_{az} is the azimuthal length scale, v is the rms velocity of the interstellar clouds and l is their mean free path. From the rotation curve of NGC 4736 published by Mulder & Van Driel (1993), the velocity gradient in the ring region is $S \sim 3.0$ km s^{-1} kpc^{-1}. The velocity dispersion in the ring is high at about 30 km/s (Mulder 1995a). If we suppose that the clouds meet at 1/4 of their full orbit and that $l \sim 500$ pc (Roberts & Hausman 1984), we find:

$\tau_{x_{az}} \sim 300$ Myr

From their simulations, Gerin et al. (1991) concluded that the inner ring is at least 1 or 2 Gyr old since it is the time scale for the formation of the outer ring observed in NGC 4736. Since the time scale obtained above is significantly shorter, azimuthal mixing by differential rotation also contribute to the small O/H dispersion observed in the star forming ring.

4.2. Radial mixing in the disc

As established previously, the slope of the global O/H gradient in the disc of NGC 4736 is significantly shallower (by about a factor of two) than that of normal spiral galaxies. In this section, we will examine two possible evolutionnary scenarios to explain this behavior.

4.2.1. The influence of the oval distortion

As revealed by observations and numerical simulations, non-axisymmetric structures like bars and oval distortions induce large-scale radial gas flows throughout galactic discs (e.g. Roberts et al. 1979; Ball 1986; Ondrechen & van der Hulst 1989; Athanassoula 1992; Friedli et al. 1994.) As said earlier, these flows homogenize the chemical composition in galaxies: abundance gradients become progressively shallower (Martin & Roy 1994, 1995; Friedli & Benz 1995). A massive oval distortion of axis ratio ~ 0.8 is present in NGC 4736 (Gerin et al. 1991; Mulder 1995b). According to the relation between the slope of the O/H gradient and the stellar bar axis ratio established by Martin & Roy (1994), the gradient in NGC 4736 should be considerably *steeper*, at least by a factor of two (see Table 6). Thus, a priori, it seems that the oval distortion cannot explain the shallow gradient of NGC 4736. Non-circular gas motions have been observed in the vicinity of the short nuclear bar but the influence of this stucture on gas kinematics in the whole disc is probably small (Möllenhoff et al. 1995). However, as discussed by Martin (1995), the *strength* of a non-axisymmetric potential like a bar is not fully described by the axis ratio; the bar mass is also important (see also Friedli & Benz 1994 and Athanassoula 1994). In the relationship found by Martin & Roy, the ratio of the bar mass to the mass shaping the axisymmetric component of the gravitationnal potential remains small ($< 10\%$) for all the (late-type) galaxies studied. However, the situation of NGC 4736 is clearly different: the oval distortion, despite its small ellipticity, is very massive in comparison to the inner disc (28% according to Möllenhoff et al. 1995). We could then expect that radial flows, certainly weaker than flows in barred galaxies but stronger than the ones observed in normal spirals, are generated in the disc of NGC 4736.

Neutral gas observations effectively confirm that weak radial streaming motions are present in the disc of NGC 4736. Strong non-circular velocities are only observed at the location of the inner ring of star formation (Buta 1988; Mulder & van Driel 1993). In the disc, the gas streaming motions appear to have radial velocities of less than 20 km/s which is significantly lower in comparison to motions observed in the disc of strong barred spirals like NGC 1365 and NGC 3359 (~ 50 km/s) (Ball 1986; Ondrechen & Van der Hulst 1989). Simulations by Friedli et al. (1994) and Friedli & Benz (1995) have shown that gas

streaming motions induced by strong bars can flatten the abundance gradient by 50% in less than 500 Myr. Thus, the timescale for homogenization of the chemical composition throughout the disc of NGC 4736 should be considerably longer.

According to Roy & Kunth (1995), the time for turbulent transport to diffuse a length scale Δx_{rad} in the radial direction is given by

$$\tau_{x_{rad}} = \frac{\Delta x_{rad}^2}{vl} \quad (2)$$

where v is the velocity of the radial flow and l is the mean free paths of the clouds. From Roberts & Hausman (1984), $l \sim 500$ pc and, for NGC 4736, Δx_{rad} = 5 kpc and $v \sim 20$ km/s. If we assume that the initial O/H gradient in NGC 4736 was steep and similar to the ones observed in normal spirals (slope $\sim -$ 0.09 dex/kpc), the time required for the radial flows induced by the oval distortion to flatten the gradient at its actual value is $\tau_{x_{rad}} \sim 1.2 \times 10^9$ years. This value is an upper limit however since the radial transport due to a bar is not a real random walk, in particular along the spiral arms where gas motions could be considered as a pure streaming flow. However, for NGC 4736, such strong streaming flows are not seen so the real time scale of radial transport of gas across the disc is probably not too far from the value derived from equation (2). It is interesting to notice that this time scale is quite similar to the time interval for which the inner and outer rings co-exist after the introduction of the non-axysimmetric potential in simulations of NGC 4736 (Gerin et al. 1991; Mulder 1995a). Thus, the presence of both rings and the shallow gradient are consistent with a scenario involving radial flows induced in the disc of NGC 4736 by the formation of the oval distortion.

4.2.2. NGC 4736: a case of seculation evolution by bars?

Following the progress made in self-consistent numerical simulations of galaxies and statistical studies, the role of bars in changing morphological types of galaxies along the Hubble sequence has received a lot of attention (see the review by Martinet 1995). It is now believed that the formation of a bar in a late-type galaxy has not only important consequences on the evolution of the disc but also on the spheroidal component (Pfenniger 1992; Friedli & Benz 1993, 1995; Norman et al. 1996). In presence of a barred structure, considerable quantities of gas coming from the disc are funneled along the bar. If the accreted gas is not completely transformed into stars in the bar, a large amount can be accumulated in the galaxy center (Martin 1996). An intense star formation activity is then triggered in the central region and newly formed stars are swept out of the galactic plane by vertical instabilities (Friedli & Benz 1995; Norman et al. 1996). This mechanism contributes to the bulge's growth. However, if sufficient mass is accumulated in the center (a few percent of the disc mass), the bar will be destroyed by dynamical instabilities. The resulting galaxy shows many morphological characteristics of an early-type spiral, in particular a very prominent bulge; furthermore, the global O/H gradient should be shallow (Friedli et al. 1994; Friedli & Benz 1995).

Could NGC 4736 represent a post-bar stage in the secular evolution of galaxies along the Hubble sequence? Although no definitive conclusion can be drawn, NGC 4736 shows several properties which are consistent with such an evolutionnary scenario. Based on a morphological study of the galaxy, Kormendy (1979) has suggested that the oval distortion could be the remains of a bar now disappeared. As stated previously, the nucleus of NGC 4736 appears to be in a "post-starburst" phase: star-formation in the central region was very active in a recent past (Walker et al. 1988; Beckman et al. 1991). According to recent simulations on the effect of bars on chemical evolution of galaxies, the O/H gradient becomes significantly shallower during the Sc $\rightarrow$ Sb transformation, a process due to the homogenizing effect of the bar (Friedli & Benz 1995); such a shallow gradient is observed in NGC 4736. The time scale to achieve this depends strongly on the rate of star-formation present in the central region of the galaxy; models by Friedli & Benz (1995) suggest that at least 1 Gyr is required. This value is consistent with the co-existence of both rings in NGC 4736. Strong bars can homogenize the chemical composition in galactic discs in $\sim$ 500 Myr (Martin & Roy 1995). As suggested by Maoz et al. (1995), NGC 4736 shows signs of a recent merger with a small galaxy. Merging processes are a very effective way to form bars and funnel gas toward central regions of galaxies (e.g. Noguchi 1988; Barnes & Hernquist 1991). Thus, NGC 4736 could represent a good example of a secular evolution of galaxies by bars along the Hubble sequence.

5. Summary

Using monochromatic imagery, we have derived the O/H abundances in a sample of 65 H II regions in the star forming ring and the disc of the RSAab(r) galaxy NGC 4736. The apparent O/H dispersion in the ringed structure is small (σ = 0.08 dex), comparable to that of the well-mixed ISM in other disc galaxies. Azimuthal mixing induced by a high rate of supernovae explosions and also by galaxy rotation can easily explain this small O/H scatter, at least if the ring was formed some 300 Myr ago or more. Numerical simulations suggest that this is the case.

Although its exact value remains incertain, the slope ($\sim -0.035 \pm 0.020$ dex/kpc) of the global O/H gradient in the disc is significantly shallower than the slope of $\sim -0.09 \pm 0.02$ dex/kpc observed in normal late-type spirals. Two scenarios appear possible: 1) The oval distortion induces weak radial flows in the disk and progressively flattens the abundance gradient. The time scale necessary for this mechanism is estimated at about 1 Gyr, in agreement with simulations of NGC 4736 suggesting that the oval distortion was formed at least 1 or 2 Gyr ago to explain the co-existence of the inner and outer rings. 2) A strong bar (possibly formed during merging with a small galaxy) was present in a recent past and has flattened the O/H gradient. This bar was destroyed by dynamical instabilities generated by the massive concentration of gas accreted in the central region which contributed to the formation of the prominent bulge actually observed in the galaxy.

Acknowledgements. We gratefully acknowledge Jean-René Roy for numerous and useful discussions and for providing the spectrum of one H II region in NGC 4736 used for the calibration of our monochromatic images. Discussions with Daniel Friedli and Robert Kennicutt were most helpful. We thank G. Turcotte, the night assistant at the Mt Mégantic Observatory, for his precious help during the observations. One of us (P.M.) was supported by NSERC (Canada) and FCAR (Québec) Postdoctoral fellowships during this work. J.B. was supported by CUSLM (University of Moncton).

References

Alloin, D., Collin-Souffrin, S., Joly, M., Vigroux, L. 1979, A&A 78, 200
Athanassoula, E. 1992, MNRAS 259, 345
Athanassoula, E. 1994, Mass-Transfer Induced Activity in Galaxies, Shlosman I. (ed.), Cambridge Univ. Press, Cambridge, p.143
Ball, R., 1986, ApJ 307, 453
Barnes, J. E., Hernquist, L. E. 1991, ApJ 370, L65
Beckman, J. E., Varela, A. M. Munoz-Tunon, C., Vilchez, J. M., Cepa, J., 1991, A&A 245, 436
Belley, J., Roy, J.-R. 1992, ApJS 87, 61
Bosma, A., van der Hulst, J. M., Sullivan, W. T. 1977, A&A 57, 373
Buta, R. J. 1984, Ph.D. Thesis, University of Texas
Buta, R. J. 1988, ApJS 66, 233
Buta, R. J. 1995, ApJS 96, 36
Combes, F., Boissé, P., Mazure, A., Blanchard, A. 1991, Galaxies et Cosmologie, InterEditions/Ed. CNRS, Paris
Condon, J. J. 1987, ApJS 65, 485
De Bruyn, A. G. 1977, A&A 54, 491
De Vaucouleurs, G., de Vaucouleurs, A., Corwin, H. G., Jr., Buta, R. J., Paturel, G., Fouqué, R. 1991, Third Reference Catalogue of Bright Galaxies, Springer Verlag, New-York
Dopita, M. A., Evans, I. N. 1986, ApJ 307, 431
Duric, N., Dittmar, M. R. 1988, ApJ 332, L67
Edmunds, M. G., 1975, ApSS 32, 483
Edmunds, M. G., Pagel, B. E. J. 1984, MNRAS 211, 507
Edmunds, M. G., Roy, J.-R., 1993, MNRAS 261, L17
Friedli, D., Benz, W. 1993, A&A 268, 65
Friedli, D., Benz, W. 1995, A&A 301, 649
Friedli, D., Benz, W., Kennicutt, R. C., 1994, ApJ 430, L105
Gerin, M., Casoli, F., Combes, F. 1991, A&A 14 251, 32
Gioia, I. M., Fabbiano, G. 1987, ApJS 63, 771
Henry, R. B. C. 1993, MNRAS261, 306
Huang, J. H., Gu, Q. S., Su, H. J., 1994, Mass-transfer induced activity in galaxies, Shlosman I. (ed.), Cambridge Univ. Press, Cambridge, p.119
Kennicutt, R. C. 1983, ApJ 272, 54
Kennicutt, R. C., Garnett, D. R. 1996, ApJ 456, 504
Klein, U., Emerson, D. T. 1981, A&A 94, 29
Kormendy, J. 1979, ApJ 227, 714
Lynds, B. T. 1974, ApJS28, 391
Maoz, D., Filippenko, A. V., Ho, L. C., Rix, H.-W., Bahcall, J. N., Schneider, D. P., Macchetto, F. D. 1995, ApJ 440, 91
Martin, P. 1992, Ph.D Thesis, Université Laval
Martin, P. 1995, AJ 109, 2428
Martin, P., 1996, Barred Galaxies, IAU Symposium No. 157, Buta R., Elmegreen B., Crocker D. (eds.), ASP, San Franscisco, p70.
Martin, P., Belley, J. 1996, ApJ, 468, 598
Martin, P., Roy, J.-R. 1992, ApJ 397, 463
Martin, P., Roy, J.-R. 1994, ApJ424, 599
Martin, P., Roy, J.-R. 1995, ApJ445, 161
Martinet, L., 1995, Fund. Cosm. Phys. 15, 141
McCall, M. L., Rybski, P. M., Shields, G. A. 1985, ApJS 57, 1
McGaugh, S. S. 1991, ApJ 380, 140
Möllenhoff, C., Matthias, M., & Gerhard, O. E. 1995, A&A 301, 359
Mulder, P. S. 1995a, A&A 303, 57
Mulder, P. S. 1995b, Ph.D Thesis, University of Groningen
Mulder, P. S., van Driel, W. 1993, A&A 272, 63
Noguchi, M. 1988, A&A 203, 259
Norman, C. A., Sellwood, J. A., Hasan, H. 1996, ApJ, in press
Oey, M. S., Kennicutt, R. C. 1993, ApJ 411, 137
Ondrechen, M. P., Van der Hulst, J. M., 1989, ApJ 342, 290
Osterbrock, D. E. 1989, Astrophysics of Gaseous Nebulae and Active Galactic Nuclei, University Science Books, Mill Valley
Pagel, B. E. J., Edmunds, M. G. 1981, ARA&A 19, 77
Pagel, B. E. J., Edmunds, M. G., Fosbury, R. A. E., Webster, B. L., 1978, MNRAS 184, 569
Pagel, B. E. J., Edmunds, M. G., Smith, G., 1980, MNRAS 193, 219
Pfenniger, D. 1992, Physics of Nearby Galaxies, Nature or Nurture?, XXVIIth Rencontres de Moriond, Thuan T.X., Balkowski C., Tran Thanh Van J. (eds.), Ed. Frontières, Gif-sur-Yvette, p.519
Pogge, R. W. 1989, ApJS 71, 433
Roberts, W. W., Huntley, J. M., van Albada, G. D. 1979, ApJ 233, 67
Roberts, W. M., Hausman, M. A. 1984, ApJ 277, 744
Roy, J.-R. 1996, Barred Galaxies, IAU Symposium No. 157, Buta R., Elmegreen B., Crocker D. (eds.), ASP, San Franscisco, p.63
Roy, J.-R., Belley, J., Dutil, Y., Martin, P. 1996, ApJ 460, 284
Roy, J.-R., Kunth, D. 1995, A&A 294, 432
Roy, J.-R., Walsh, J. R., 1996, MNRAS, submitted
Ryder, S. 1995, ApJ 444, 610
Sandage, A. 1961, The Hubble Atlas of galaxies, Carnegie Institution of Washington, Washington, DC
Sandage, A., Bedke, J. 1994, The Carnegie Atlas of Galaxies (Washington, D.C.: Carnegie Institution of Washington)
Savage, B. D., Mathis, J. S. 1979, ARA&A 17, 73
Scowen, P. A., Dufour, R. J., Hester, J. J. 1992, AJ 104, 92
Shaw, M. A., Combes, F., Axon, D. J., Wright, G. S., 1993, A&A 273, 31
Tenorio-Tagle, G. 1996, AJ,
Tully, R. B. 1988, Nearby Galaxies Catalog, Cambridge Univ. Press, Cambridge
Van der Kruit, P. C. 1971, A&A 15, 110
Vila-Costas, M. B., Edmunds, M. G. 1992, MNRAS 259, 121
Wada, K., Habe, A. 1992, MNRAS 258, 82
Walker, C. E., Lebofsky, M. J., Rieke, G. H. 1988, ApJ 325, 687
Walsh, J. R., Roy, J.-R. 1989, ApJ 341, 722
Wozniak, H., Friedli, D., Martinet, L., Martin, P., Bratschi, P., 1995, A & AS 111, 115
Wray, J. D. 1988, The Color Atlas of Galaxies, Cambridge Univ. Press, Cambridge
Zaritsky, D., Kennicutt, R. C., Huchra, J. P. 1994, ApJ 420, 87

This article was processed by the author using Springer-Verlag LaTeX A&A style file *L-AA* version 3.